Am J Transl Res 2021;13(1):73-87
www.ajtr.org /ISSN:1943-8141/AJTR0116505

Original Article

Compound TDB (Tricyclic decyl benzoxazole) induces autophagy-dependent apoptosis in the gastric cancer cell line MGC-803 by regulating PI3K/AKT/mTOR

Min Xiao[1,2,3*], Chunhua Lin[4*], Zhaoxin Yang[1,2,3], Shuhong Tian[1,2,3], Yanan Huang[1], Jian Fu[1]

[1]Hainan Medical College Preclinical Pharmacology Laboratory, Hainan, P. R. China; [2]Center for Drug Safety Evaluation Research of Hainan Province, Hainan, P. R. China; [3]Hainan Provincial Key Laboratory of Preclinical Pharmacology and Toxicology, HaiKou 571199, Hainan, P. R. China; [4]Guo Rui Yinuo Drug Safety Evaluation and Research Co., Ltd. Xixian New Area, Xian Yang 712000, Shaanxi, P. R. China. [*]Equal contributors.

Received June 17, 2020; Accepted October 8, 2020; Epub January 15, 2021; Published January 30, 2021

Abstract: Objective: Gastric cancer is a potential malignant tumor. Extensive research has shown that apoptosis and autophagy are important mechanisms of cancer pathogenesis. This study aimed to explore the role and mechanism of TDB in apoptosis and autophagy in MGC-803 cells. Methods: In cell experiments, the proliferation, apoptosis and autophagy of MGC-803 cells were evaluated by the MTT assay, TUNEL, flow cytometry, MDC, and TEM. Through molecular experiments, the TDB-induced apoptosis and autophagy effects were evaluated by examining the levels of Cleaved-PARP/PARP, Cleaved-caspase3/procaspase3, Beclin-1, p62 and the ratio of LC3-II/LC3-I. At the animal level, the anti-tumor effect of TDB *in vivo* was evaluated by assessing tumor volume and bioluminescence value. Results: Regarding mechanism, TDB induces apoptosis and autophagy through PI3K/AKT/mTOR. At the same time, more importantly, TDB promotes 3-methyladenine or autophagy activator rapamycin-mediated. The induced proliferation inhibition and pro-apoptosis effect, which inhibit autophagy and induce an increase in apoptosis. Conclusion: TDB may up-regulate PARP, Cleaved Caspase-3, Beclin1 and LC3B and down-regulate the expression of P62 and other apoptosis and autophagy genes through the activation of PI3K/AKT/mTOR pathway signalling proteins, leading to autophagy-dependent apoptosis. At the animal level, TDB has good anti-tumor efficacy in vivo. In summary, TDB has potential anti-tumor efficacy *in vivo* and *in vitro*.

Keywords: TDB, MGC-803 cells, autophagy, apoptosis, PI3K/AKT/mTOR pathway

Introduction

As a common human malignant tumor type in humans, gastric cancer has high morbidity and mortality rates worldwide [1]. The current treatment methods are mainly surgical resection and drug treatment, which have their own limitations due to metastasis or the development of drug resistance [2-4]. Therefore, the search for potential chemotherapeutic drugs is on-going.

During tumorigenesis, normal cells gain the ability to evade programmed cell death, which allows them to grow indefinitely. Molecular targeted therapy, which is able to specifically inhibit tumors through inhibiting proliferation, apoptosis and autophagy, has become increasingly popular. During the process of apoptosis, cytochrome c is released from the mitochondria into the cytoplasm, which then initiates apoptosis. Finally, cytochrome c promotes increased numbers of apoptotic bodies in the cytoplasm and increases the levels of downstream caspase enzymes. This reaction promotes caspase-3, -8 and -9 cleavage, efficient poly (adenosine diphosphate) ribose polymerase (PARP) cleavage and activation, and apoptosis via external and internal pathways. As another key type of cellular self-digestion, autophagy has a dual role induced autophagic death [5, 6]. Autophagy is able to maintain homeostasis of the cell environment, promote cell proliferation and inhibit apoptosis; however, autophagy also clears accumulated mutations from the mitochondria, triggering apoptosis.

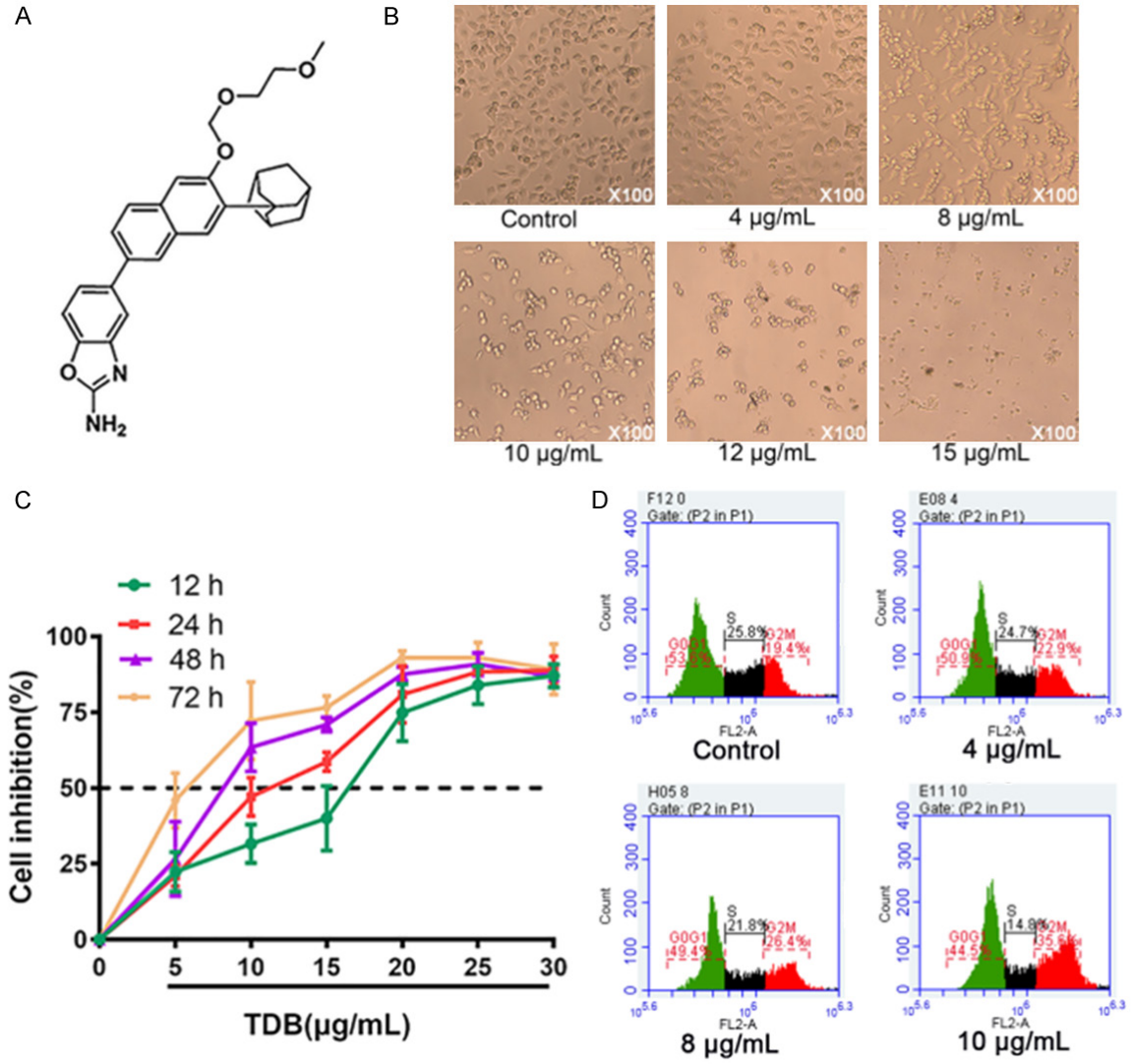

Figure 1. TDB inhibits the proliferation of MGC-803 cells. A. Chemical structure of TDB. B. Morphological changes of MGC-803 cells induced by TDB treatment, 100× magnification. C. The effect of TDB on MGC-803 cell proliferation activity. D. The influence of TDB on the cell cycle of MGC-803 cells.

Benzoxazole compounds are a class of benzoheterocyclic compounds that have anti-inflammatory, antibacterial and antitumor effects. These compounds are able to act as mTOR inhibitors and tyrosine kinase inhibitors to exert antitumor effects. TDB is a chemically synthesized derivative of benzoxazole (**Figure 1A**). The results of previous studies by our group have indicated that TDB inhibits the proliferation and promotes the apoptosis of MGC-803 cells. However, the mechanism by which TDB affects the proliferation, autophagy and apoptosis of MGC-803 cells and the interrelation of these effects has remained largely elusive. Therefore, the present study focused on exploring the antitumor activity of TDB and the mechanisms that induce cell apoptosis and autophagy at the molecular, cellular and *in vivo* or ganism levels.

Materials and methods

Major reagents and instruments

The human gastric cancer MGC-803 cell line was purchased from the Shanghai Cell Bank of the Chinese Academy of Sciences (Shanghai, China). Mycoplasma detection kits (C0298S), fetal bovine serum, basal medium, trypsin and 3-methyladenine (3-MA) were purchased from Thermo Fisher Scientific, Inc. MTT (cat. no.

ST316), 5-ethynyl-2'-deoxyuridine (EdU; cat. no. C0075S) kits, terminal deoxynucleotidyl transferase deoxyuridine triphosphate nick-ending (no. C1086) and Hoechst (cat. no. C0003) kits, SDS-PAGE gel preparation kit (cat. no. P00-12AC), rapamycin (cat. no. S1842) and antibodies to autophagy-related 5 (cat. no. AF2269) were obtained from Biyuntian Biotechnology Research Institute. The Annexin V-FITC/PI apoptosis kit (cat. no. 556547) was purchased from BD Biosciences. Polyvinylidene PVDF membranes were obtained from EMD Millipore. The monodansy lcadaverine (MDC) kit (cat. no. DA0041) was purchased from Beijing Leagen Biotechnology Co., Ltd. PARP (cat. no. 9532), cleaved caspase-3 (cat. no. 9661), Bax (cat. no. 5023), Bcl-2 (cat. no. 3498), GAPDH (cat. no. 5174), Beclin1 (cat. no. EPR19662), P62 (cat. no. EPR4844), ATG5 (cat. no. AF2269), PI3K (110A) (cat. no. 4249), PI3K (p85) (cat. no. 4228), p-AKT (Ser473) (cat. no. 4060), P-AKT (Thr308) (cat. no. 13038), AKT (cat. no. 4685), p-mTOR (cat. no. 5536) and mTOR (cat. no. 2972) were diluted at a ratio of 1:1,000, and LC3B (cat. no. EPR18709) was diluted at a ratio of 1:2,000. The membranes were washed with Tris-buffered saline containing Tween-20 (TBST) and then incubated with horseradish peroxidase-conjugated rabbit IgG (cat. no. ARG65351; 1:10,000 dilution, Abcam) as the secondary antibody at 4°C in a refrigerator shaker for 12 h.

MTT assay

MGC-803 cells (37°C in a humidified atmosphere with 5% CO_2) were seeded in a 96-well plate (approximately 10^5) for 24 h and were treated with different concentrations of TDB. A negative control was included and the blank control group was adjusted to zero. The optical density value at 492 nm was measured using a microplate reader. The experiment was repeated 3 times using six wells for each concentration. The concentration and growth inhibition curves were drawn and IC_{50} values at 12, 24, 48 and 72 h were determined.

EdU assay

MGC-803 cells (approximately 10^5) were seeded in a 6-well plate, inoculated for 48 h and then treated with TDB for 24 h and an EdU working solution for 2 h. Subsequently, the cells were Permeate (P0097) fixed for 15 min at room temperature, incubated with click additive reagent for 30 min at room temperature, washed with PBS and counterstained with a Hoechst kit. Fluorescence microscopy was used to measure the fluorescence excitation wavelengths of 346 and 555 nm. The experiment was repeated 3 times.

Flow cytometric assays.

The cells (approximately 10^5) were seeded in a 6-well plate and cultured for 48 h before drug treatment. After a 24 h drug treatment, the cells were collected, washed and transformed into a single-cell suspension. Precooled binding buffer (1 mL) was added. The samples were divided into four tubes and 5 μL of Annexin V-FITC and propidium iodide (PI) was added prior to 15 min incubation at room temperature in the dark. Subsequently, flow cytometry was used to detect the apoptosis rate of each experimental group. The experiment was repeated 3 times.

A single-cell suspension was seeded in a 6-well plate (approximately 10^5) and TDB was added for 24 h. The cells were collected to prepare single-cell suspensions. The cell suspensions were fixed with prechilled 75% ethanol (4°C) for 24 h and PI was then added, followed by incubation at 4°C for 30 min. Finally, the cell cycle distribution in each experimental group was detected by flow cytometry. The experiment was repeated 3 times.

Hoechst detection of apoptosis

MGC-803 cells were seeded into 6-well plates (approximately 10^5) and then treated with drugs for 24 h. The cells were then washed and fixed with Immune fixative (P0098) for 10 min at room temperature and then 0.5 mL of Hoechst 33258 staining solution was added, followed by incubation at room temperature for 10 min in the dark. After washing with PBS, the cells were observed and images were captured under a fluorescence microscope. The experiment was repeated 3 times.

TUNEL detection of apoptosis

The cells (approximately 10^5) were treated with different concentrations of TDB and then incubated with fixing solution for 20 min, washed with permeabilization solution for 5

min, washed with 100 μl of TUNEL working solution and incubated at 37°C for 1 h. Subsequently, the slides were mounted with an autofluorescence quenching solution. The cells were observed and images were acquired under a fluorescence microscope. The experiment was repeated 3 times.

TEM

MGC-803 cells were treated with TDB (10 μg/mL). After 24 h, cell suspensions were collected for glutaraldehyde fixation. The cells were fixed in1% osmic acid, rinsed with PBS fixed again with 1% osmium acid for 3 h and rinsed with PBS. The samples were stored in a 4°C refrigerator following a gradient washing with 50% ethanol 70% ethanol 90% ethanol 90% ethanol + 90% ethylene glycol, at room temperature and 100% formaldehyde. The film was observed under a TEM at 500 nm-2 μm.

MDC assay

A single-cell suspension was seeded into a 96-well plate (approximately 10^5). TDB was applied at different concentrations for 24 h. 1× MDC was added for incubation at 37°C for 30 min. After 3 washes, the autophagosomes were observed under a fluorescence microscope and images were acquired. The experiment was repeated 3 times.

Western blotting analysis

TDB group, LY294002, 3-MA, and rapamycin were combined with TDB for 24 h. Total protein was collected by lysis with 2% SDS lysate buffer and the protein concentration was determined with a bicinchoninic acid kit. Total protein (20 μg) was then subjected to 6-10% SDS-PAGE and transferred to a PVDF membrane. Following incubation with 5% skimmed milk powder, the samples were incubated at 4°C for 12 h with the following primary antibodies (Rabbit mAb, monoclonal) The membrane was washed with Tris-buffered saline containing Tween-20 (TBST) and then incubated with horseradish peroxidase-conjugated rabbit IgG (cat. no. ARG65351; 1:10,000 dilution) as the secondary antibody at 4°C in a refrigerated shaker for 12 h. The membrane was washed with TBST and developed by chemiluminescence (P0018S/GelDoc XR+). The experiment was repeated 3 times.

Immunofluorescence assay

Paraffin sections were subjected to gradient transparent elution and were used for antigen repair. The sections were then incubated with a primary antibody (1:200, 4°C) overnight and incubated with a fluorescent secondary antibody (goat anti-rabbit or goat anti-mouse 1:100 dilution) for 2 h at room temperature. After washing, the samples were sealed. Images were acquired at excitation wavelengths of 315-488 nm to observe the expression of autophagy and apoptosis-associated proteins [7, 8].

Xenograft experiment in nudemice

The animal experiments were reviewed and approved by the Experimental Animal Management and Use Committee of the Hainan Provincial Center for Drug Safety Evaluation and Research (Safety assessment of medicine saving [2016] No. 001). Nude mice (18-22 g, 4-6 w) were injected subcutaneously with 0.1 mL of MGC-803 cells (approximately 10^8) to construct a subcutaneous tumor transplant model of human gastric cancer. Subsequently, the mice were housed in a SPF barrier environment for 2 weeks. The temperature was maintained at 20-26°C, the relative humidity was 40-70%, and the light/dark cycle was 12/12 h alternating light and dark. When the tumor diameters reached 1-2 cm, the animals were randomly assigned according to their body weight into the following 5 groups (6 mice per group): control group, cisplatin group and TDB groups. The TDB groups were administered 50, 100 or 200 mg/kg TDB solution intragastrically by oral gavage once a day for 21 consecutive days; the control group was administered an equal volume of 0.9% sodium chloride; and the cisplatin group was given seven tail-vein injections of 0.4 mg/mL cisplatin once every 2 days, with a recovery period of 14 days. During the experiment, the body weight and tumor volumes were measured. The luminescence value for tumor growth was measured once a week with a small animal *in vivo* imaging system. At the end of the experiment, the animals were euthanized (130 mg/kg pentobarbital sodium) and the tumor tissues were removed. The tumor weights were determined and the tissues were immersed in 4% formaldehyde and fixed (20°C) for pathological histological examination.

Table 1. The effect of TDB on cell cycle arrest of MGC-803 cells (%)

C (μg/mL)	G0/G1	S	G2/M
Control	57.35±6.32	21.91±6.73	19.80±0.62
4	53.05±3.83	23.43±4.80	22.50±1.59##
8	51.93±4.51	20.91±2.72	25.60±2.53*,##
10	45.09±4.70	17.22±4.79	35.24±0.76**,##

Note: Compared with the control group, *indicates $P < 0.05$, **indicates $P < 0.01$, compared with the 10 μg/mL group, ##indicates $P < 0.01$.

Tumor histology

Sections of gastric cancer tumors from the xenograft experiment were cleared with xylene and an alcohol gradient; stained with hematoxylin, acidic ethanol and eosin; and dehydrated, cleared, air-dried and sealed with neutral resin. The slides were mounted and the histomorphology changes were observed under an optical microscope.

Statistical analysis

SPSS 22.0 (IBM Corp.) was used for statistical analyses. The weight, volumes and bioluminescence value were used to test for homogeneity of variance and perform one-way analysis of variance. The values are expressed as the mean ± standard deviation. Comparisons between groups of cell viability, flow cytometry and western blotting, body weight, volume and bioluminescence value of nude mice were analysed via ANOVA followed by a Student Newman-Keuls post hoc test. Mann-Whitney U-test for non-parametric procedures was used to determine microhardness and mineral apposition rate. $P < 0.05$ was considered to indicate a statistically significant difference.

Results

TDB inhibits the proliferation of MGC-803 cells

The results of the MTT assay suggested that treatment of MGC-803 cells with different concentrations of TDB (0, 5, 10, 15, 20, 25 and 30 μg/mL) for 12, 24, 48 and 72 h was able to inhibit cell proliferation in a concentration- and time-dependent manner (**Figure 1B**, **1C**). The IC_{50} value was 10.68 μg/mL at 24 h. Thereafter, the concentrations of TDB used to treat MGC-803 cells were set to 0, 4, 8 and 10 μg/mL in the subsequent experiments. The results of the EdU assay (Figure S1) also suggested that the cell replication ability was limited, and the number of dead cells increased with increasing TDB concentration.

TDB blocks the cell cycle of MGC-803 cells

Flow cytometry was used to determine the cell cycle distribution of MGC-803 cells treated with different concentrations of TDB (0, 4, 8 and 10 μg/mL) for 24 h. As presented in **Figures 1D**, S2 and **Table 1**, TDB caused cell cycle arrest of the cells at the G2/M phase [9-11]. Compared with the negative control group (19.8%), the percentage of cells in the G2/M phase in the TDB 4, 8 and 10 μg/mL treatment groups increased in a concentration-dependent manner (22.5, 25.6 and 35.2%, respectively), and the S-phase population decreased in turn.

TDB induces apoptosis in MGC-803 cells

The Hoechst method was used to observe the morphology of cells treated with TDB. As presented in **Figures 2A** and S3, the nuclear structure of the control group was normal with weak and uniform blue fluorescence, while the nuclei in the TDB treatment group were partially condensed with dense staining and bright blue fluorescence. The results of the TUNEL assay indicated that the cells in the control group had a clear structure and a relatively uniform distribution. Round apoptotic cells in the TDB group were stained dark red and increased with increasing in number drug concentration. Flow cytometry was used to detect apoptosis and the results are presented in **Figures 2B** and S4. Compared with the control group, the late apoptotic rate in the TDB treatment group increased significantly to 38.8% in a concentration-dependent manner ($P < 0.05$). In addition, apoptosis-associated proteins were detected by immunoblotting **Figure 2C**, **2D**. Compared with the control group, the expression levels of cleaved caspase-3, Cleaved-PARP and Bax were significantly increased in the TDB 10 μg/mL group ($P < 0.05$), PARP and Procaspase-3 were not significantly affected Bcl-2 was decreased and the Bax/Bcl-2 ratio was increased, Cleaved-PARP/PARP, and Cleaved caspase-3/procaspase-3 were increased. The above results indicated that TDB promoted cell apoptosis through the mitochondrial pathway.

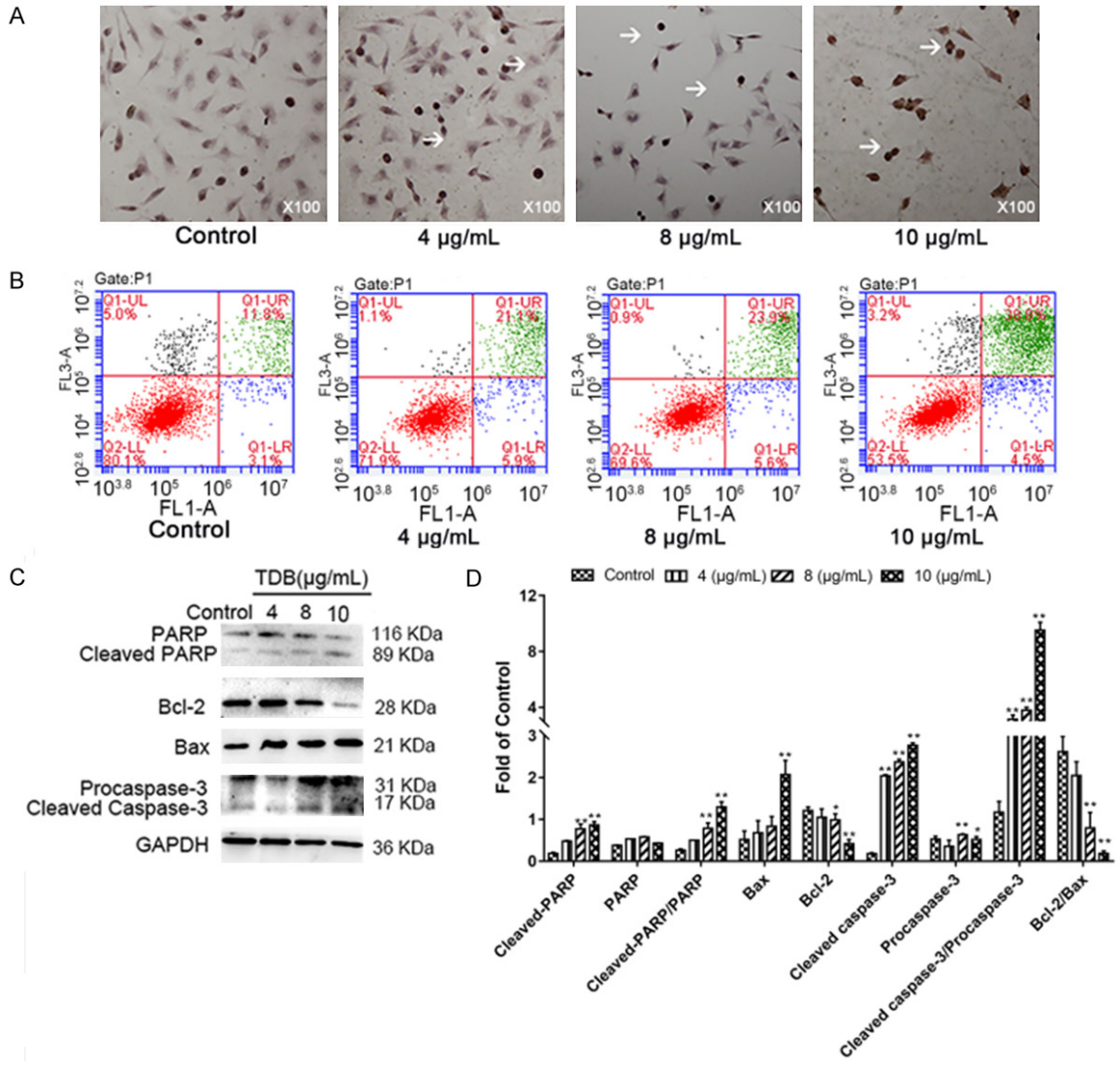

Figure 2. TDB-induced apoptosis of MGC-803 cells. Apoptosis was evaluated by (A) the terminal deoxynucleotidyl transferase deoxyuridine triphosphate nick-end labelling method and (B) flow cytometry, 100× magnification. (C) Western blot analysis and pair-wise comparison using the S-N-K method. (D) Histogram of the expression levels of apoptosis-associated proteins, and pairwise comparison using S-N-K method. $^{*}P < 0.05$, $^{**}P < 0.01$ vs. the Control group. PARP, poly (adenosine diphosphate) ribose polymerase.

TDB induces autophagy in MGC-803 cells

To detect whether TDB is able to induce autophagy in cells, the MDC assay was employed. As shown in Figure S5, after TDB treatment, the MGC-803 cells were subjected to staining and exhibited dense, yellowish-green granules of different sizes. With increasing TDB concentrations, the number of stippled particles increased significantly. At the same time, autophagy marker proteins were assessed by immunoblotting. As presented in **Figure 3A**, **3B**, compared with the control, TDB treatment significantly increased Beclin1, ATG5 and LC3II expression and decreased P62 protein expression. Furthermore, the LC3II/LC3I ratio increased. To further confirm whether autophagosomes were formed after the MGC-803 cells were treated with TDB, TEM was performed (**Figure 3C**). Compared with the control group, the morphology of the cells in the TDB group showed autophagic vacuoles, autophagic vesicles and autophagosomes and increased lysosomes. However, lysosomes were increased. The above results indicated that TDB is able to induce autophagy in MGC-803 cells.

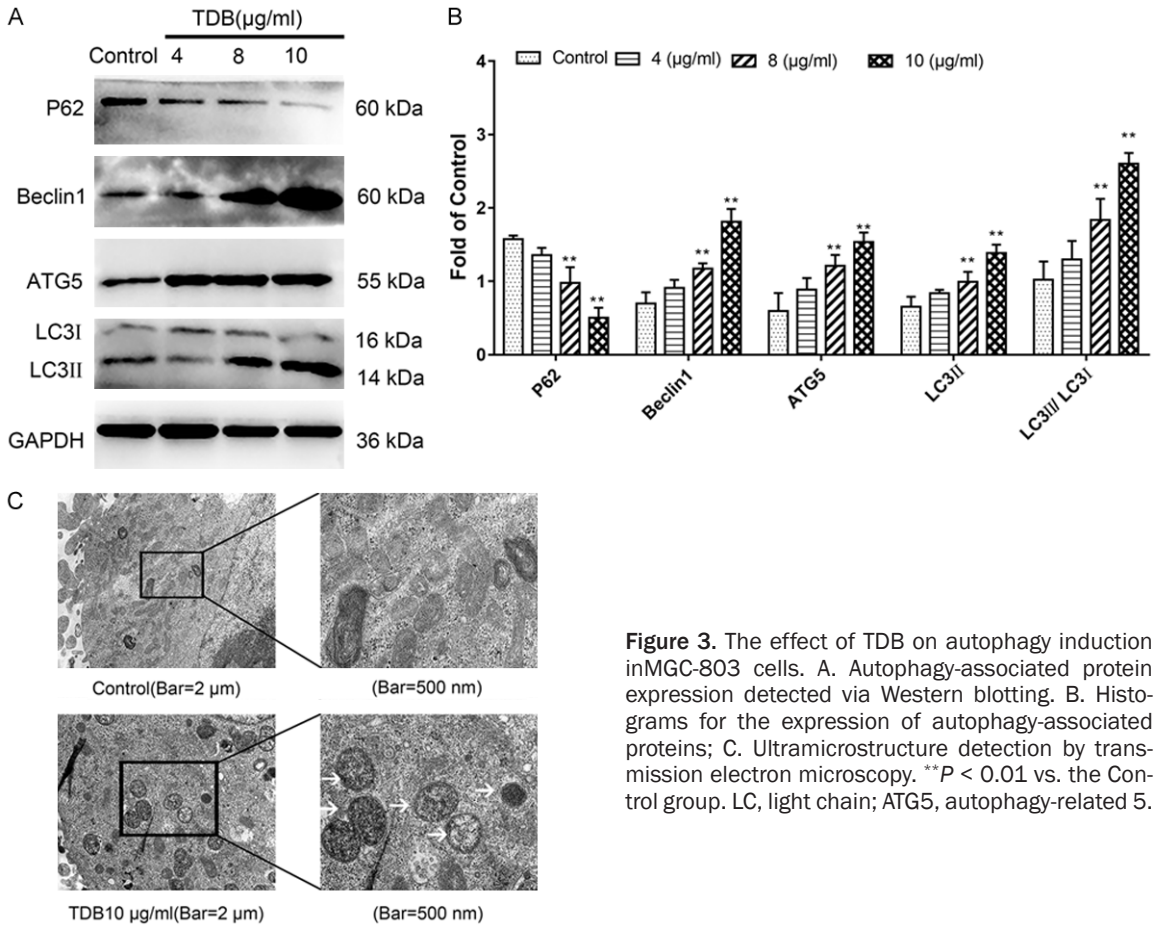

Figure 3. The effect of TDB on autophagy induction inMGC-803 cells. A. Autophagy-associated protein expression detected via Western blotting. B. Histograms for the expression of autophagy-associated proteins; C. Ultramicrostructure detection by transmission electron microscopy. $^{**}P < 0.01$ vs. the Control group. LC, light chain; ATG5, autophagy-related 5.

TDB may regulate apoptosis through the PI3K/AKT/mTOR pathway

PI3K/AKT/mTOR is a signalling pathway closely linked to cell autophagy and apoptosis [12, 13]. This pathway is involved in the mediation of multiple signalling pathways, including cell transcription, translation, proliferation and survival [14]. PI3K class I is activated mainly by insulin receptors, including the regulatory subunit P85 and the auxiliary subunit P110. After PI3K is activated by growth signals on the plasma membrane, it inhibits AKT and mTOR complex 1 activation, thereby inhibiting autophagy and apoptosis [15]. The expression of PI3K/AKT/mTOR pathway-associated proteins was detected in cells after 24 h of treatment with TDB **Figure 4A**, **4B**. Compared with the control group, the levels of PI3K (p85), p-Akt (Ser473), p-Akt (Thr308), p-mTOR, p-Akt (Ser473), p-Akt (Ser473)/total Akt, p-Akt (Thr308)/total Akt were not significantly decreased and exhibited a certain concentration dependence, while the protein expression of total Akt, PI3K (p110α), mTOR and Procaspase-3 was not significantly affected. The expression of PI3K/AKT/mTOR pathway-associated proteins was detected in cells after a 24 h of treatment with TDB and the results are shown in **Figure 5A**, **5B**. Compared with the TDB group, the protein levels of PI3K (p85), p-Akt (Thr308) and p-Akt (Ser473) were significantly reduced in the combined treatment group, the ratio of PI3K (p85)/PI3K (p110α), p-Akt (Thr308)/Akt, p-Akt (Ser473)/Akt and p-mTOR/mTOR were significantly reduced, and the levels of cleaved caspase-3 and Cleaved caspase-3/procaspase-3 were significantly increased ($P < 0.05$). These results indicated that TDB-induced cell apoptosis may be mediated by the PI3K/AKT/mTOR pathway.

Inhibition of autophagy enhances TDB-induced apoptosis

Previous experiments have confirmed that TDB is able to induce cell autophagy and apoptosis [16, 17], but the mechanisms of the interaction

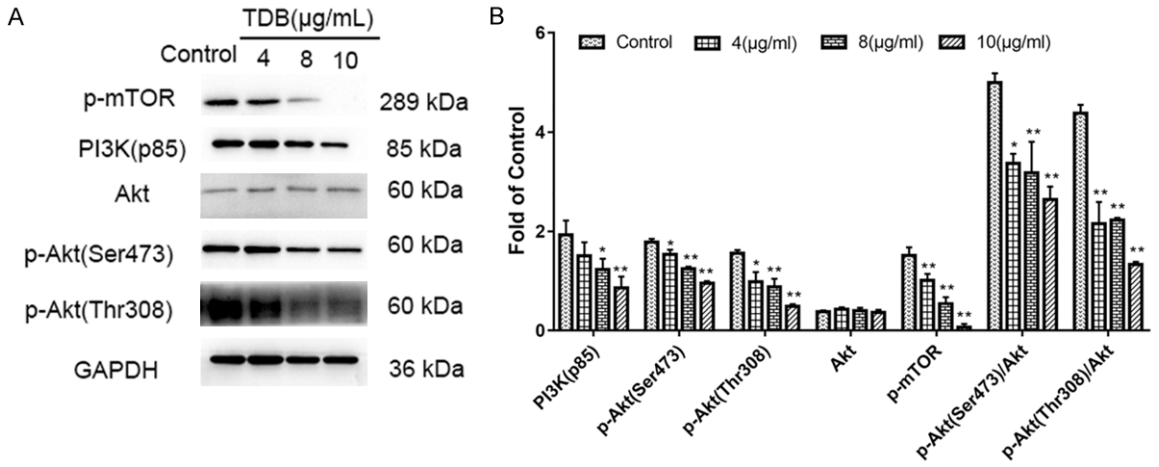

Figure 4. TDB inhibits the PI3K/Akt/mTOR pathway. A. Immunoblotting detection of the expression of PI3K/Akt/mTOR pathway-associated proteins; B. Histograms of the expression of PI3K/Akt/mTOR pathway-associated proteins. $^{*}P < 0.05$, $^{**}P < 0.01$ vs. Control group, p-Akt, phosphorylated Akt.

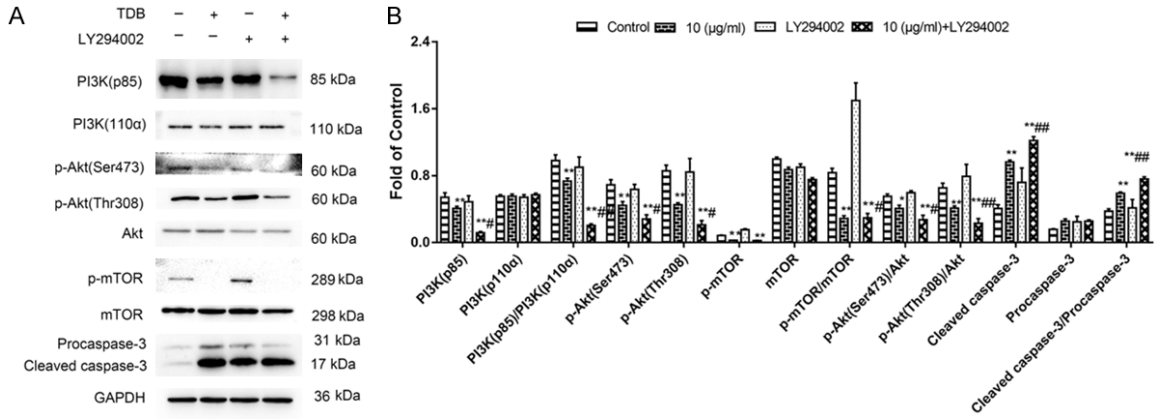

Figure 5. TDB inhibits the PI3K/Akt/mTOR pathway to increase apoptosis. A. Detection by immunoblotting. B. Histograms for the expression of PI3K/Akt/mTOR pathway and apoptosis-associated proteins. $^{*}P < 0.05$, $^{**}P < 0.01$ vs. control group, $^{\#}P < 0.05$, $^{\#\#}P < 0.01$ vs. thecombined treatment group.

between the two pathways remain to be clarified. To observe the effect of TDB-induced autophagy on apoptosis, the autophagy inhibitor 3-MA was used to interfere with autophagy and the effect on apoptosis was determined. The results of the Hoechst staining assay are provided in **Figure 6A**. Compared with the TDB group alone, the 3-MA and TDB treatment group had densely stained nuclei and partially condensed nuclei, exhibiting obvious bright blue fluorescence, indicating increased apoptosis. The flow cytometry results indicated that the apoptotic rate of 3-MA and the blank group showed no obvious change, while the TDB group showed increased apoptosis compared with that in the control group (28.5%), and the combined treatment group showed significantly increased apoptosis (48.5%) ($P < 0.01$; **Figure 6B**, **6C**). The results of the immunoblotting analysis of autophagy-associated proteins represented in **Figures 6D** and S6. Compared with blank group, the expression of Beclin1, ATG5 and LC3II in the combined treatment group decreased, while the expression of P62 was upregulated. Furthermore, although PARP increased, the levels of cleaved caspase-3 and Cleaved-PARP were significantly increased. At the same time, Cleaved-PARP/PARP and Cleaved caspase-3/procaspase-3 were increased. The above results indicated that autophagy inhibition may enhance TDB-induced apoptosis.

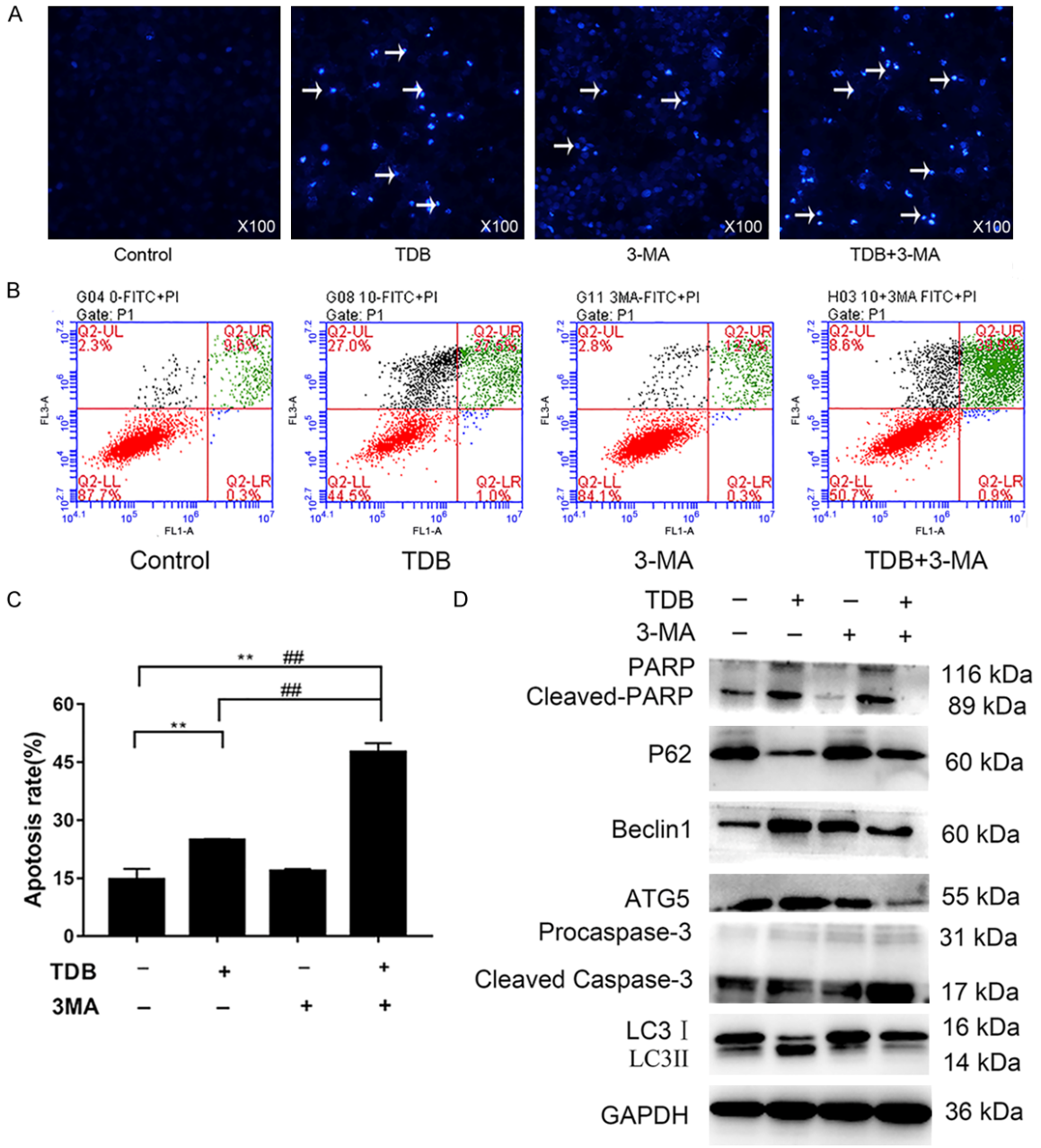

Figure 6. Inhibition of autophagy enhances TDB-induced apoptosis. (A) Apoptosis detected with the Hoechst method, 100× magnification. (B) Flow cytometry was used to detect apoptotic cells. (C) A histogram of the apoptosis rate was generated from (B). (D) Immunoblotting analysis was used to detect autophagy and apoptosis-associated protein expression. $^{**}P < 0.01$ vs. Control group, $^{\#\#}P < 0.01$ vs. the combined treatment group.

Rapamycin, an mTOR inhibitor, is able to inhibit the phosphorylation of mTOR [18]. The cells were treated with rapamycin in combination with TDB, and Hoechst, TUNEL and flow cytometry assays were used to detect apoptosis. The Hoechst staining results indicated that the cells in the combined treatment group were densely stained and the number of blue granules was significantly increased (Figure S7). Following TUNEL staining, certain cells in the combined treatment group were stained bright green and this staining increased with increasing concentrations (Figure S8). The flow cytometry results indicated that the apoptosis rate in the combination group reached 78.4%, which was significantly higher than that in the control group and the TDB group alone ($P < 0.01$; **Figure 7A**, **7B**). The Western blotting results suggested that,

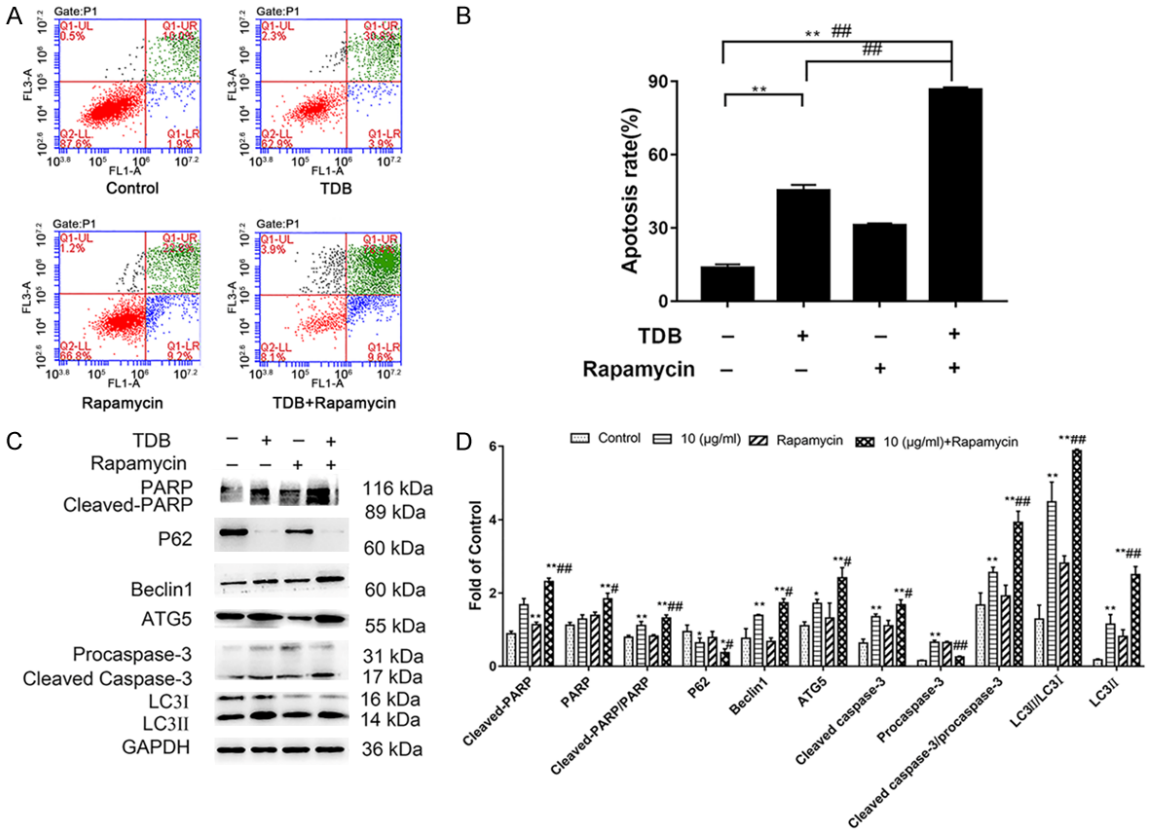

Figure 7. Inhibition of autophagy enhances TDB-induced apoptosis via inhibition of mTOR phosphorylation. (A) Flow cytometry was used to detect apoptosis. (B) A histogram of the apoptosis rate was generated from (A). (C) Immunoblotting was used to detect cell phagocytosis and apoptosis-associated protein expression. (D) Histogram of the protein expression determined by Western blotting $^{*}P < 0.05$, $^{**}P < 0.01$ vs. control group, $^{\#}P < 0.05$, $^{\#\#}P < 0.01$ vs. the combined treatment group. ATG5, autophagy-related 5; LC, light chain; PARP, poly (adenosine diphosphate) ribose polymerase.

compared with the TDB alone treatment group, P62 protein expression was downregulated in the rapamycin-treated group, while Beclin1, ATG5, LC3II and LC3d n1, expression increased, and cleaved-PARP and Cleaved caspase-3 are activated upon cleavage, and although protein levels of PARP, Procaspase-3 were increased, the ratio of Cleaved-PARP/PARP, and Cleaved caspase-3/procaspase-3 were Significantly increased (**Figure 7C**, **7D**). In summary, TDB may regulate apoptosis by inhibiting mTOR protein phosphorylation via the PI3K/AKT/mTOR pathway [19, 20].

TDB has antitumor effects in vivo

In the animal experiment, no significant differences in the bodyweights of the nude mice were observed between the TDB treatment group and the control group ($P > 0.05$). A small-animal *in vivo* imaging system was used to monitor tumor growth in the nude mice. As presented in **Figures 8A-C**, S9 and **Tables 2-4**, compared with the control group, the tumor volume, weight and chemiluminescence values were significantly decreased in the TDB treatment group ($P < 0.05$). The tumor tissues were sectioned and stained with H&E. Microscopy observation revealed that the tumor tissue cells in the control group had mostly normal structures and were distributed in clusters. However, the cells in the TDB treatment group were decreased in size, exhibited nuclear shrinkage and displayed apoptosis (**Figure 8D**). At the same time, TUNEL staining in the TDB treatment group was positive with brown-yellow precipitation and the staining degree became deeper and more intense with increasing TDB concentrations (Figure S10). In addition, immunofluorescence was used to detect apoptosis and autophagy-associated protein expression in tumor tissues. The results indicated that, compared with the control group, the TDB treat-

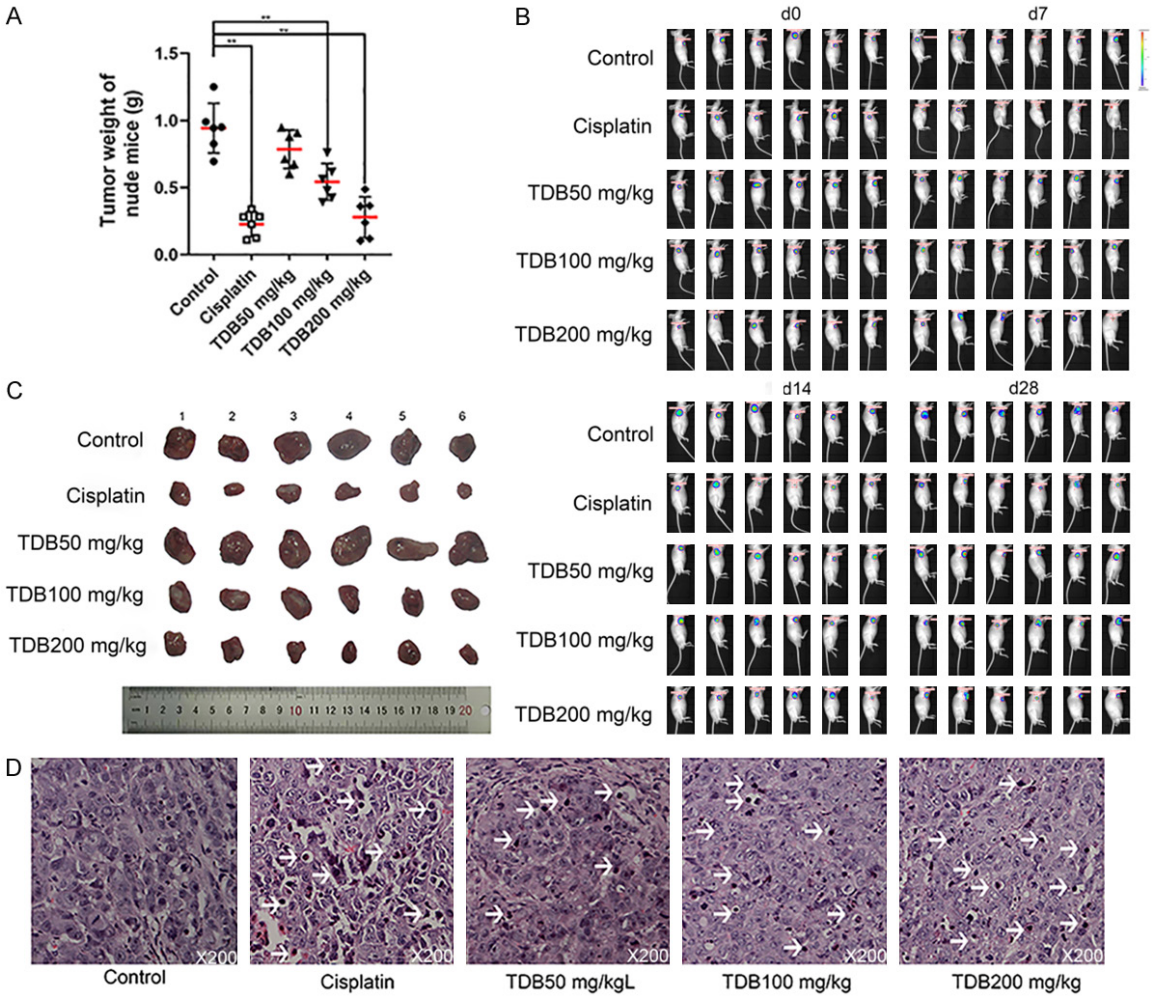

Figure 8. TDB has an antitumor effect in vivo. A. The weight of transplanted tumors. Pairwise comparison using S-N-K method. B. A small-animal live imaging system was used to monitor tumor growth in vivo in real time. C. Subcutaneous tumortissue of MGC-803 cells. D. H&E staining and terminal deoxynucleotidyl transferase deoxyuridine triphosphate nick-end labelling staining of paraffin sections of tumor tissue, 100× magnification. **p < 0.01 vs. the control group.

Table 2. The effect of TDB on the weight of subcutaneously transplanted tumors in nude mice (g)

Group	d0	d7	d14	d28
Control	20.4±1.6	21.2±2.3	22.0±2.2	19.5±3.2
Cisplatin	20.9±1.0	20.4±0.8	17.4±0.7**	16.9±0.5
TDB 50 mg/kg	21.7±1.2	22.1±1.7	21.7±2.3	21.8±2.2
TDB 100 mg/kg	19.6±1.4	20.1±1.1	20.9±1.3	19.6±2.2
TDB 200 mg/kg	20.7±1.4	22.0±2.1	21.8±2.7	22.3±2.7*

Note: Compared with the control group, *indicates $P < 0.05$, **indicates $P < 0.01$.

ment group had significantly enhanced fluorescence intensities for Beclin1; ATG5, LC3II, PARP and Bax, P62 and Bcl-2. These proteins were all clearly expressed, ATG5, LC3II, PARP, Bax levels were upregulated while P62 and Bcl-2 levels were downregulated (Figure S11). The above results indicated that TDB has an antitumor effect *in vivo* and that the mechanism of tumor suppression is associated with apoptosis and autophagy.

Discussion

In the present study, TDB was shown to inhibit MGC-803 cell proliferation, block the cells in G2/M phase, and induce apoptosis and autophagy. The effects of TDB on the induction of autophagy and apoptosis in MGC-

Table 3. The effect of TDB on the volume of subcutaneous xenografts in nude mice (mm^3)

Group	d0	d7	d14	d28
Control	312.81±51.50	364.77±102.49	631.50±163.63	682.17±186.31
Cisplatin	273.52±43.63	251.88±58.70*	88.64±52.83**	117.99±100.91**
TDB 50 mg/kg	277.72±32.61	255.84±88.85	212.09±66.03**	266.09±70.61**
TDB 100 mg/kg	232.92±55.94	330.08±129.66	228.27±147.26**	267.16±163.07**
TDB 200 mg/kg	263.93±64.50	217.57±76.30*	92.09±77.67**	191.00±199.95**

Note: Compared with the control group, *indicates $P < 0.05$, **indicates $P < 0.01$.

Table 4. The effect of TDB on the luminous value of nude mice subcutaneous xenografts ($\times 10^8$ p/sec/cm^2/sr)

Group	d0	d7	d14	d28
Control	5.9±4.9	6.8±4.2	17.2±7.7	41.1±32.3
Cisplatin	7.6±4.3	8.4±6.3	8.7±7.9	1.7±1.3**
TDB 50 mg/kg	7.1±9.4	6.5±4.4	10.8±7.5	13.9±20.3**
TDB 100 mg/kg	8.3±1.4	12.5±19.9	6.8±4.9*	5.4±1.8**
TDB 200 mg/kg	8.8±7.4	8.4±9.4	4.5±2.0**	3.1±4.5**

Note: Compared with the control group, *indicates $P < 0.05$, **indicates $P < 0.01$.

803 cells were further investigated. The key signalling pathways that regulate apoptosis and autophagy as well as the upstream PI3K/AKT/mTOR pathway, were examined. The results suggested that TDB-induced apoptosis in MGC-803 cells may depend on the PI3K/AKT/mTOR signalling pathway and that inhibition of autophagy promoted apoptosis in cells.

Induction of apoptosis is one of the methods ways by which antitumor drugs promote cell death [21]. The Hoechst staining and flow cytometry results of the present study suggested that TDB significantly increased the apoptotic ratio. As a key pro-apoptotic protein in early mitochondrial apoptosis, Bax oligomerizes with Bcl-2 homologous antagonist killer after receiving an apoptotic signal and forms holes in the mitochondrial membrane to increase its permeability, resulting in a decrease in membrane potential. As a result, apoptotic factors are released into the cytoplasm and the apoptotic pathway is activated by downstream caspase-level enzyme-associated reactions [22]. Bcl-2 is another key protein that mediates apoptosis. After forming a heterodimer, Bcl-2 and Bax participate in mitochondrial pore repair and reduce permeability to exert an antiapoptotic role. PARP is a downstream marker of apoptosis in cells and its cleavage is able to activate caspase-3 activity and finally induce cell apoptosis [23-28]. In the present study, the immunoblotting results indicated that TDB regulated apoptosis by increasing the Bax/Bcl-2 ratio; at the same time, caspase-3 and PARP cleavage were significantly increased. The above results indicated that TDB is able to induce MGC-803 cell apoptosis through the mitochondrial pathway [29].

TEM is the gold standard for detecting autophagy [30-32]. Observation of the ultrastructure of cells in the TDB treatment group revealed an incomplete cell structure, increased mitochondria, Golgi apparatus swelling, increased cytoplasm, disrupted cell membranes, autophagy vesicles, autophagosomes, and autolysosomes with double membrane structures. Dansylcadaverine is a specific autophagosome marker [33]. As a means of autophagy detection, the results of the MDC assay revealed that yellow-green particles increased in the cells treated with TDB and dense staining appeared. These results suggested that TDB induces autophagy in MGC-803 cells. Beclin1, P62, ATG5 and LC3 are important proteins associated with the induction of autophagy. In this process, a complex form between Beclin1 and VPS34, and ATG14 is responsible for recruiting responsible autophagy proteins and initiating autophagy. P62 is a polyubiquitinated binding protein. LC3 also participates in ubiquitination to form LC3I and is then lapidated to form LC3II, which may be used as a marker of autophagosome degradation. ATG5-ATG12 is a key fusion protein, the formation of which is involved in the process of autophagic vesicle elongation. Microtubule-associated LC3 is a marker protein for the formation and extension of the biphasic membranes of autophagosomes, and the degree of autophagy is reflected by the LC3II/LC3I transformation status. The ratio of LC3II/LC3I is positively correlated with the number of autoph-

agic vesicles. The immunoblotting results of the present study indicated that LC3II protein expression was upregulated, LC3I protein was downregulated and the conversion of LC3I to LC3II was increased. Furthermore, P62 protein was degraded and Beclin1 and ATG5 expression was increased upon treatment with TDB. The above results indicated that TDB is able to induce autophagy in MGC-803 cells in a concentration-dependent manner.

The inhibition of autophagy is able to enhance apoptosis [34-37]. In the present study, after cells were treated with the autophagy inhibitor 3-MA combined with TDB, the Hoechst and Annexin V/PI staining results suggested that the apoptotic ratio was increased. The autophagy inhibitor 3-MA inhibits the occurrence of autophagy. The upregulation of P62 and downregulation of Beclin1, ATG5 and LC3II suggested that autophagy was inhibited, while the cleavage of the apoptotic proteinscaspase-3 and PARP was increased. These results indicated that apoptosis was enhanced and suggested that autophagy has a protective role against TDB-induced MGC-803 cell death. By inhibiting autophagy, the antitumor effect of TDB is augmented.

In conclusion, the present study demonstrated that TDB is able to inhibit the proliferation of MGC-803 cells and induce apoptosis and autophagy. This apoptosis induction may be exerted via the PI3K/AKT/mTOR pathway. Inhibiting autophagy was also able to enhance apoptosis. Furthermore, TDB exhibited good antitumor activity *in vivo*, and therefore may be a novel providing a potential targeted drug for the treatment of gastric cancer.

Acknowledgements

This research was funded by the Hainan Provincial Drug Innovation Service Platform (No. ZDKJ2016001-2). This study was approved by the Experimental Animal Management and Use Committee of the Research Center for Drug Safety Evaluation of Hainan Province.

Disclosure of conflict of interest

None.

Address correspondence to: Jian Fu, Basic College of Hainan Medical College, Hainan Medical College, Longhua District, Haikou City College Road, Haikou 571500, Wanning, Hainan, P. R. China. E-mail: fujian.hnmc@163.com

References

[1] Zhou XT, Pu ZJ, Liu LX, Li GP, Feng JL, Zhu HC and Wu LF. Inhibition of autophagy enhances adenosineinduced apoptosis in human hepatoblastoma HepG2 cells. Oncol Rep 2019; 41: 829-838.

[2] Jolly MK, Somarelli JA, Sheth M, Biddle A, Tripathi SC, Armstrong AJ, Hanash SM, Bapat SA, Rangarajan A and Levine H. Hybrid epithelial/mesenchymal phenotypes promote metastasis and therapy resistance across carcinomas. Pharmacol Ther 2019; 194: 161-184.

[3] Gill JG, Piskounova E and Morrison SJ. Cancer, oxidative stress, and metastasis. Cold Spring Harb Symp Quant Biol 2016; 81: 163-175.

[4] Chen ZH, Qi JJ, Wu QN, Lu JH, Liu ZX, Wang Y, Hu PS, Li T, Lin JF, Wu XY, Miao L, Zeng ZL, Xie D, Ju HQ, Xu RH and Wang F. Eukaryotic initiation factor 4A2 promotes experimental metastasis and oxaliplatin resistance in colorectal cancer. J Exp Clin Cancer Res 2019; 38: 196.

[5] Levine B and Klionsky DJ. Development by self-digestion: molecular mechanisms and biological functions of autophagy. Dev Cell 2004; 6: 463-477.

[6] Mizushima N, Levine B, Cuervo AM and Klionsky DJ. Autophagy fights disease through cellular self-digestion. Nature 2008; 451: 1069-1075.

[7] Surace M, DaCosta K, Huntley A, Zhao W, Bagnall C, Brown C, Wang C, Roman K, Cann J, Lewis A, Steele K, Rebelatto M, Parra ER, Hoyt CC and Rodriguez-Canales J. Automated multiplex immunofluorescence panel for immuno-oncology studies on formalin-fixed carcinoma tissue specimens. J Vis Exp 2019; 21: 143.

[8] Lightbody ED and Nicol CJB. Immunofluorescence labeling of nuclear receptor expression in formalin-fixed, paraffin-embedded tissue. Methods Mol Biol 2019; 1966: 101-105.

[9] Lin YT, Wang HC, Hsu YC, Cho CL, Yang MY and Chien CY. Capsaicin induces autophagy and apoptosis in human nasopharyngeal carcinoma cells by downregulating the PI3K/AKT/mTOR pathway. Int J Mol Sci 2017; 18: 1343.

[10] Wang Y, Deng X, Yu C, Zhao G, Zhou J, Zhang G, Li M, Jiang D, Quan Z and Zhang Y. Synergistic inhibitory effects of capsaicin combined with cisplatin on human osteosarcoma in culture and in xenografts. J Exp Clin Cancer Res 2018; 37: 251.

[11] Wang Y, Xu W, Yan Z, Zhao W, Mi J, Li J and Yan H. Metformin induces autophagy and G0/G1

phase cell cycle arrest in myeloma by targeting the AMPK/mTORC1 and mTORC2 pathways. J Exp Clin Cancer Res 2018; 37: 63.
[12] Sun Z, Zheng L, Liu X, Xing W and Liu X. Sinomenine inhibits the growth of melanoma by enhancement of autophagy via PI3K/AKT/mTOR inhibition. Drug Des Devel Ther 2018; 12: 2413-2421.
[13] Wang SS, Chen YH, Chen N, Wang LJ, Chen DX, Weng HL, Dooley S and Ding HG. Hydrogen sulfide promotes autophagy of hepatocellular carcinoma cells through the PI3K/Akt/mTOR signaling pathway. Cell Death Dis 2017; 8: e2688.
[14] Dadashpour S, Kucukkilinc TT, Ercan A, Hosseinimehr SJ, Naderi N and Irannejad H. Synthesis and anticancer activity of Benzimidazole/Benzoxazole substituted triazolotriazines in hepatocellular carcinoma. Anticancer Agents Med Chem 2019; 19: 2120-2129.
[15] Desai S, Desai V and Shingade S. In-vitro anticancer assay and apoptotic cell pathway of newly synthesized benzoxazole-N-heterocyclic hybrids as potent tyrosine kinase inhibitors. Bioorg Chem 2019; 94: 103382.
[16] Xie WY, Zhou XD, Yang J, Chen LX and Ran DH. Inhibition of autophagy enhances heat-induced apoptosis in human non-small cell lung cancer cells through ER stress pathways. Arch Biochem Biophys 2016; 607: 55-66.
[17] Liu W, Wang X, Liu Z, Wang Y, Yin B, Yu P, Duan X, Liao Z, Chen Y, Liu C, Li X, Dai Y and Tao Z. SGK1 inhibition induces autophagy-dependent apoptosis via the mTOR-Foxo3a pathway. Br J Cancer 2017; 117: 1139-1153.
[18] El-Helby AA, Sakr H, Eissa IH, Abulkhair H, Al-Karmalawy AA and El-Adl K. Design, synthesis, molecular docking, and anticancer activity of benzoxazole derivatives as VEGFR-2 inhibitors. Arch Pharm (Weinheim) 2019; 352: e1900113.
[19] Kresty LA, Weh KM, Zeyzus-Johns B, Perez LN and Howell AB. Cranberry proanthocyanidins inhibit esophageal adenocarcinoma in vitro and in vivo through pleiotropic cell death induction and PI3K/AKT/mTOR inactivation. Oncotarget 2015; 6: 33438-33455.
[20] Sarbassov DD, Guertin DA, Ali SM and Sabatini DM. Phosphorylation and regulation of Akt/PKB by the rictor-mTOR complex. Science 2005; 307: 1098-1101.
[21] Burgess DJ. Apoptosis: refined and lethal. Nat Rev Cancer 2013; 13: 79.
[22] Lee HJ, Saralamma VVG, Kim SM, Ha SE, Raha S, Lee WS, Kim EH, Lee SJ, Heo JD and Kim GS. Pectolinarigenin induced cell cycle arrest, autophagy, and apoptosis in gastric cancer cell via PI3K/AKT/mTOR signaling pathway. Nutrients 2018; 10: 1043.
[23] Po WW, Thein W, Khin PP, Khing TM, Han KWW, Park CH and Sohn UD. Fluoxetine simultaneously induces both apoptosis and autophagy in human gastric adenocarcinoma cells. Biomol Ther (Seoul) 2019; 28: 202-210.
[24] Wang L, Zhu Z, Han L, Zhao L, Weng J, Yang H, Wu S, Chen K, Wu L and Chen T. A curcumin derivative, WZ35, suppresses hepatocellular cancer cell growth via downregulating YAP-mediated autophagy. Food Funct 2019; 10: 3748-3757.
[25] Li J, Fu Y, Hu X and Xiong Y. Psoralidin inhibits the proliferation of human liver cancer cells by triggering cell cycle arrest, apoptosis and autophagy and inhibits tumor growth in vivo. J BUON 2019; 24: 1950-1955.
[26] Li R, Wang X, Zhang X, Yu J, Feng J, Lv P, Lou Y and Chen Y. Ad5-EMC6 mediates antitumor activity in gastric cancer cells through the mitochondrial apoptosis pathway. Biochem Biophys Res Commun 2019; 513: 663-668.
[27] Liu JZ, Hu YL, Feng Y, Guo YB, Liu YF, Yang JL, Mao QS and Xue WJ. Rafoxanide promotes apoptosis and autophagy of gastric cancer cells by suppressing PI3K/Akt/mTOR pathway. Exp Cell Res 2019; 385: 111691.
[28] Liu Y and Fan D. Ginsenoside Rg5 induces G2/M phase arrest, apoptosis and autophagy via regulating ROS-mediated MAPK pathways against human gastric cancer. Biochem Pharmacol 2019; 168: 285-304.
[29] Lin X, Han L, Weng J, Wang K and Chen T. Rapamycin inhibits proliferation and induces autophagy in human neuroblastoma cells. Biosci Rep 2018; 38: BSR20181822.
[30] Wu ST, Sun GH, Cha TL, Kao CC, Chang SY, Kuo SC and Way TD. CSC-3436 switched tamoxifen-induced autophagy to apoptosis through the inhibition of AMPK/mTOR pathway. J Biomed Sci 2016; 23: 60.
[31] Mei L, Sang W, Cui K, Zhang Y, Chen F and Li X. Norcantharidin inhibits proliferation and promotes apoptosis via c-Met/Akt/mTOR pathway in human osteosarcoma cells. Cancer Sci 2019; 110: 582-595.
[32] Wang RC, Wei Y, An Z, Zou Z, Xiao G, Bhagat G, White M, Reichelt J and Levine B. Akt-mediated regulation of autophagy and tumorigenesis through Beclin 1 phosphorylation. Science 2012; 338: 956-959.
[33] Yuan CX, Zhou ZW, Yang YX, He ZX, Zhang X, Wang D, Yang T, Wang NJ, Zhao RJ and Zhou SF. Inhibition of mitotic Aurora kinase A by alisertib induces apoptosis and autophagy of human gastric cancer AGS and NCI-N78 cells. Drug Des Devel Ther 2015; 9: 487-508.
[34] Yan W, Ma X, Zhao X and Zhang S. Baicalein induces apoptosis and autophagy of breast cancer cells via inhibiting PI3K/AKT pathway in vivo and vitro. Drug Des Devel Ther 2018; 12: 3961-3972.

[35] Li W, Zhou Y, Yang J, Li H, Zhang H and Zheng P. Curcumin induces apoptotic cell death and protective autophagy in human gastric cancer cells. Oncol Rep 2017; 37: 3459-3466.

[36] Pan Y, Gao Y, Chen L, Gao G, Dong H, Yang Y, Dong B and Chen X. Targeting autophagy augments in vitro and in vivo antimyeloma activity of DNA-damaging chemotherapy. Clin Cancer Res 2011; 17: 3248-3258.

[37] Zhang P, Lai ZL, Chen HF, Zhang M, Wang A, Jia T, Sun WQ, Zhu XM, Chen XF, Zhao Z and Zhang J. Curcumin synergizes with 5-fluorouracil by impairing AMPK/ULK1-dependent autophagy, AKT activity and enhancing apoptosis in colon cancer cells with tumor growth inhibition in xenograft mice. J Exp Clin Cancer Res 2017; 36: 190.

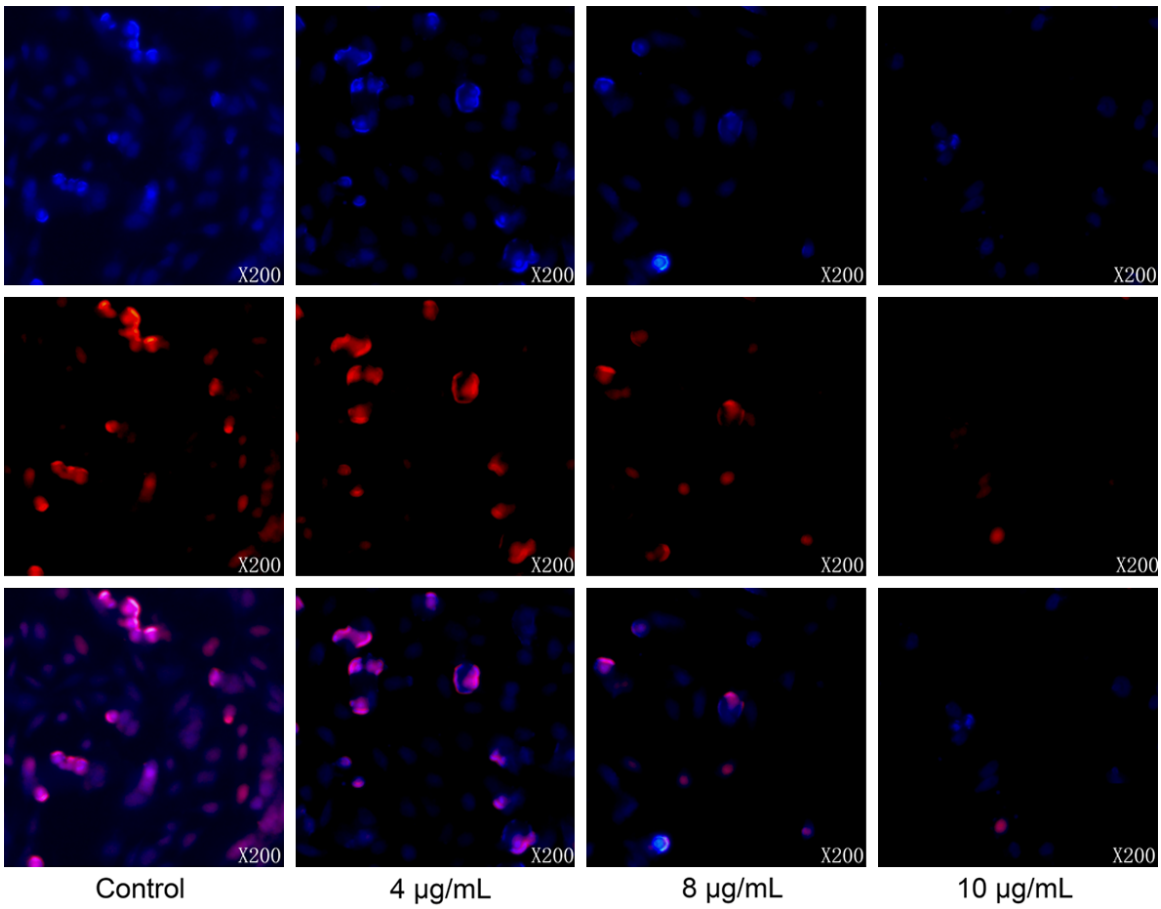

Figure S1. TDB inhibits the proliferation of gastric cancer MGC-803 cell, 200× magnification.

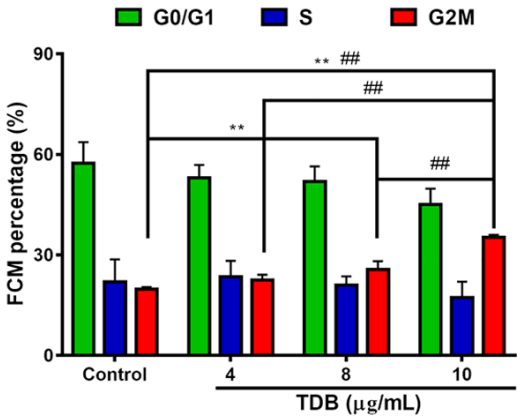

Figure S2. Histogram of the expression levels of cell cycle.

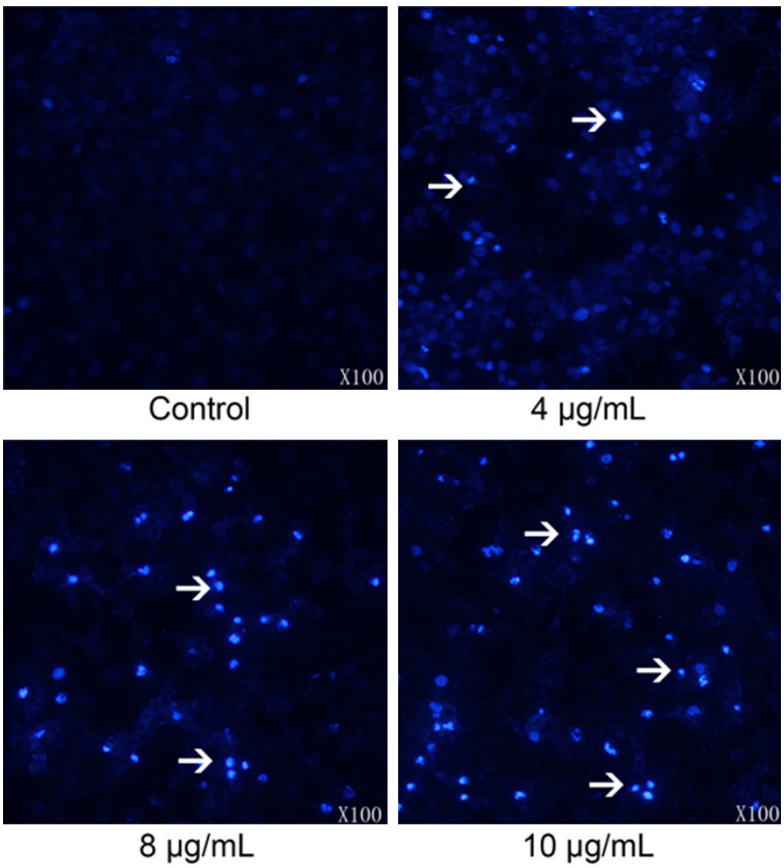

Figure S3. Apoptosis detected with the Hoechst method, 100× magnification.

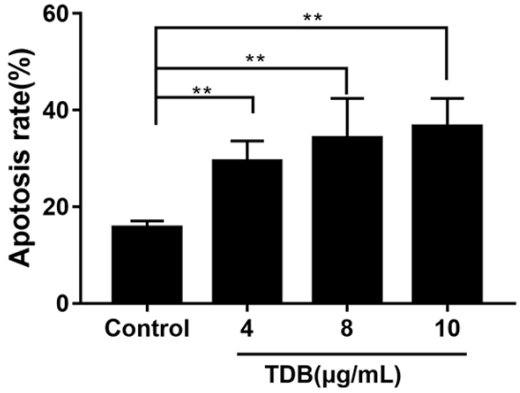

Figure S4. Histogram of the expression levels of Apotosis rate.

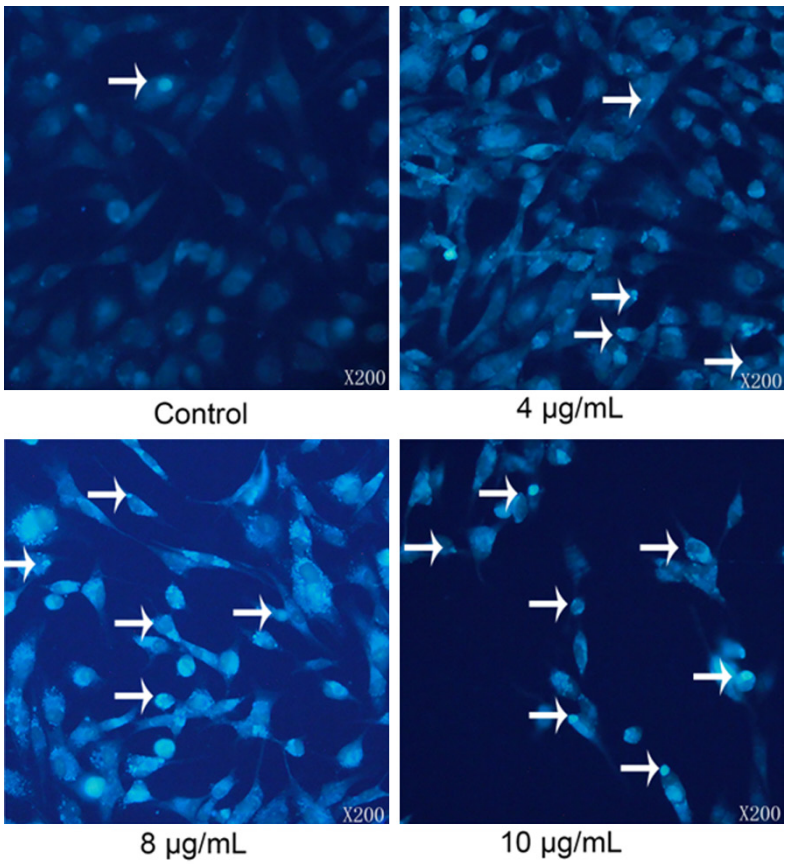

Figure S5. Ultramicrostructure detection by MDC, 100× magnification.

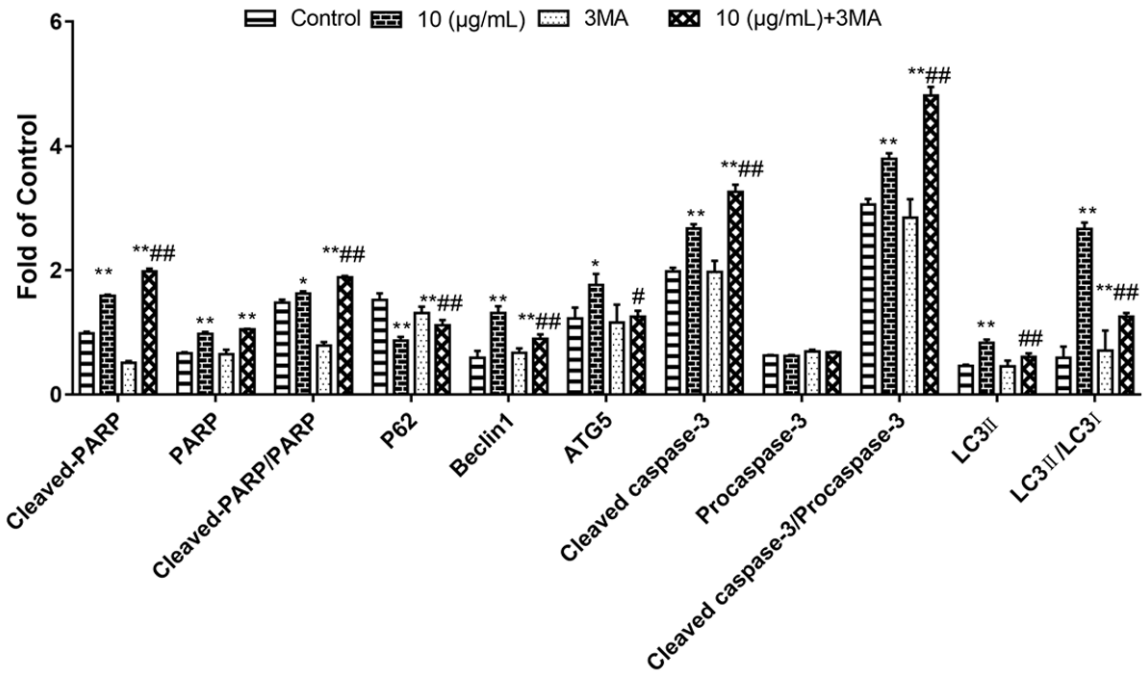

Figure S6. Histogram of the protein expression determined by western blotting $^{*}P<0.05$, $^{**}P<0.01$ vs. control group, $^{\#}P<0.05$, $^{\#\#}P<0.01$ vs. The combined treatment group. ATG5, autophagy-related 5; LC, light chain; PARP, poly (adenosine diphosphate) ribose polymerase.

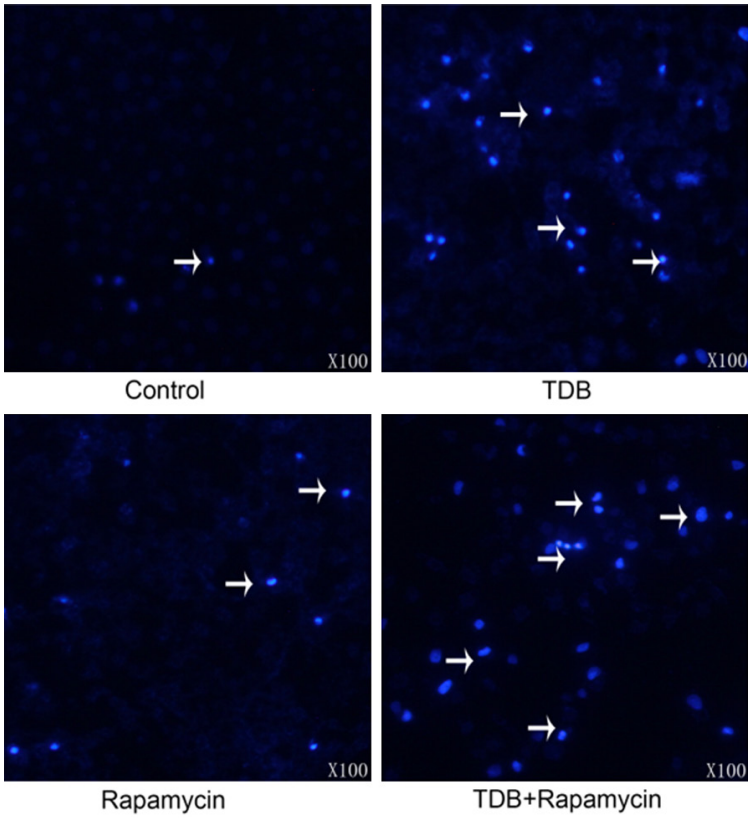

Figure S7. Apoptosis detected with the Hoechst method, 100× magnification.

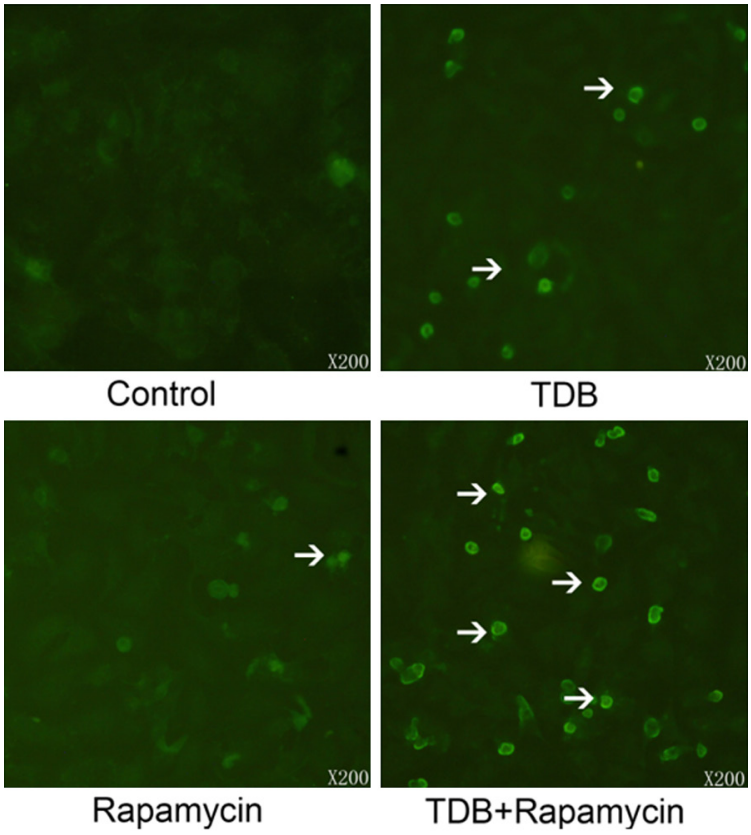

Figure S8. Apoptosis detected with the Tunel method, 200× magnification.

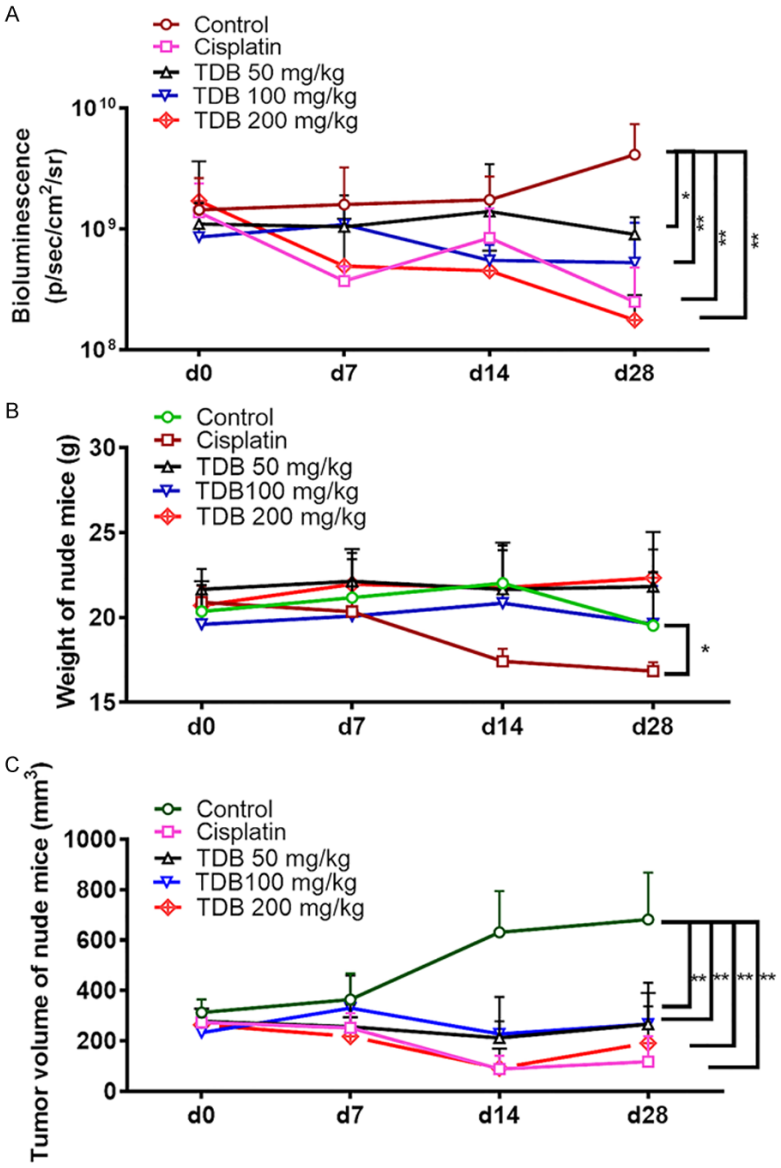

Figure S9. Testing related indicators of nude mice. A. 4-week bioluminescence trend graph of subcutaneous xenograft tumor in nude mice. B. 4 weeks weight gain trend of subcutaneous transplanted tumor in nude mice. C. Growth trend of tumor volume in nude mice subcutaneously transplanted tumors at 4 weeks.

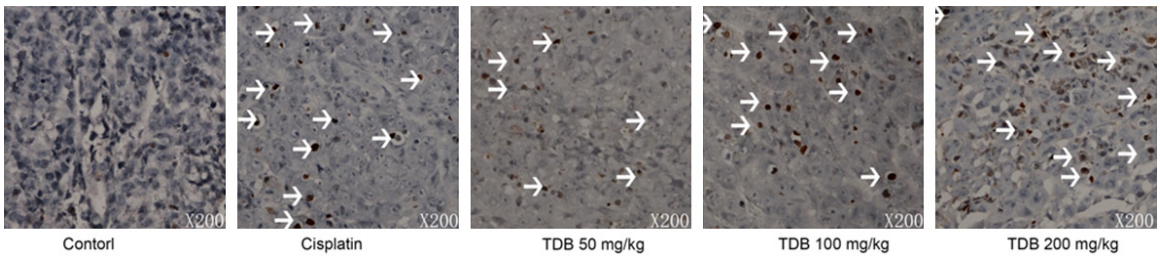

Figure S10. Tunel staining and terminal deoxynucleotidyl transferase deoxyuridine triphosphate nick-end labelling staining of paraffin sections of tumor tissue, 200× magnification.

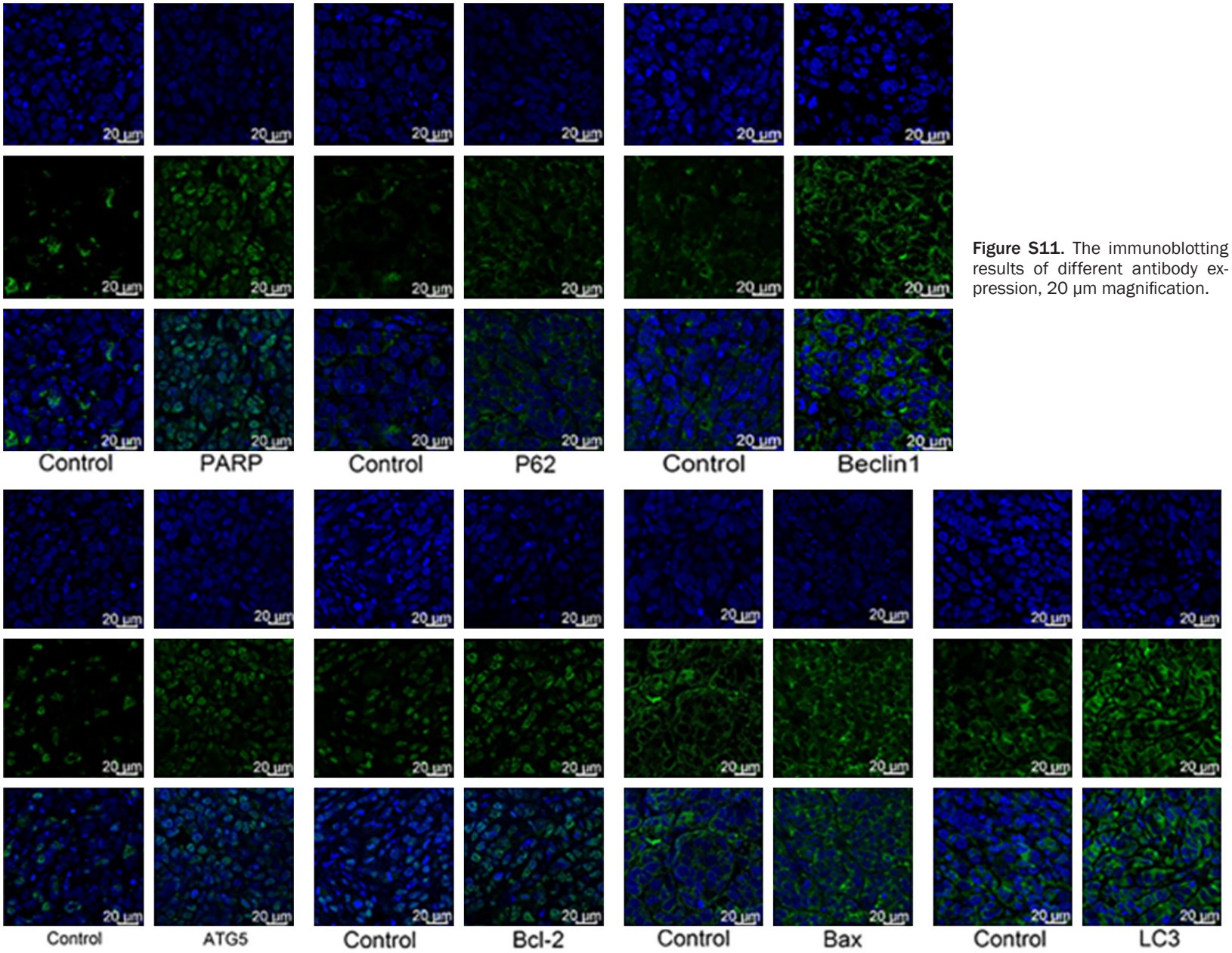

Figure S11. The immunoblotting results of different antibody expression, 20 μm magnification.